Preprint Title	Laser Ablation of 2D Layered Materials to Synthesize Metastable Nanostructures
Authors	Sepideh Khalili, Najma Khatoon, Mark Sulkes, Gregory Guisbiers and Douglas B. Chrisey
Publication Date	06 März 2025
Article Type	Full Research Paper
ORCID® iDs	Sepideh Khalili - https://orcid.org/0009-0006-7363-3521

Laser Ablation of 2D Layered Materials to Synthesize Metastable Nanostructures

Sepideh Khalili[1], Najma Khatoon[1], Mark Sulkes[2], Grégory Guisbiers[3] and Douglas B. Chrisey[1]

Department of Physics and Engineering Physics, Tulane University, New Orleans Louisiana, 70118

Department of Chemical and Biomolecular Engineering, Tulane University, New Orleans Louisiana, 70118

Department of Physics & Astronomy, University of Arkansas at Little Rock, Little Rock, AR, 72204

Abstract

Pulsed Laser Ablation in Liquids (PLAL) is a technique for synthesizing high-purity, ligand-free nanomaterials with controlled size and morphology. This study focuses on the synthesis of MXene nanostructures (Ti_3C_2), by using a focused pulsed excimer laser at 193 nm and 2-4 J/cm^2 (150 mJ at 5 Hz for 30 minutes). Using a 2 mm thick and 5 mm diameter Ti_3C_2 target in a solvent blend of deionized water and dodecyl sulfate dispersant, producing nanostructured MXenes under transient conditions of ~2,000 K temperature and 10^7-10^8 Pa pressure. The method minimizes contamination from precursors and byproducts, offering precise control over nanoparticle size and distribution while preserving structural integrity and functional properties. The synthesized MXenes were characterized using Scanning Electron Microscopy (SEM) and Energy Dispersive Spectroscopy (EDS) and revealed distinct morphologies such as wrinkled sheet-like structures like graphene oxide, uniform nanostructures consistent 2D flakes indicating a controlled synthesis that yields thin, uniform layers WS_2, and minimal synthesis damage: low defect density and minimal oxidation observed in EDS spectra. This study demonstrates the viability of PLAL method for producing high-quality MXene nanoparticles and provides a foundation for future innovations in nanomaterial synthesis for a wide range of other 2D technological applications.

1. Introduction

Nanomaterials are widely studied for their unique properties, including high surface-to-volume ratio, tunable electronic behavior, and enhanced catalytic performance, which make them valuable for applications in energy storage, catalysis, and electronics. However, traditional synthesis techniques like chemical vapor deposition, sol-gel processes, and ball milling often struggle to achieve high purity, structural precision, and scalability.

Pulsed Laser Ablation in Liquids (PLAL) offers a clean and efficient alternative for nanomaterial synthesis. This technique uses high-energy laser pulses to ablate a solid target submerged in liquid, producing nanostructures with well-controlled size, shape, and composition. PLAL is particularly advantageous for stabilizing metastable phases, which are difficult to achieve through conventional methods, enabling the fabrication of nanomaterials with superior properties for advanced applications[1,2].

When high-energy photons are absorbed by a material, they excite electrons to higher energy states. The subsequent decay of these excited states leads to the emission of thermal energy, which can be harnessed as ablation for various applications. In the context of PLAL, pulsed photonic energy absorption initiates the ablation process by creating hot plasma (~10,000–15,000 K) which leads to the vaporization of the target material. This absorption and rapid decay of photonic energy play a crucial role in determining the size, shape, and properties of the resulting nanoparticles [3].

Traditional synthesis methods, including chemical approaches, physical techniques, and gas-phase methods, have already been widely employed; however, PLAL has emerged as a particularly effective technique for producing exceptional purity, ligand-free nanomaterials [4]. PLAL offers several distinct advantages over conventional methods, such as the ability to synthesize metastable nanophases and nanoparticle colloids characterized by exceptional stability and purity [4]. For

example, stable platinum nanoparticles were synthesized via PLAL in water without surfactants like SDS, as hydroxyl groups naturally stabilized the particles and prevented aggregation [5], Moreover, PLAL is capable of trapping metastable phase transformations and material reshaping via the rapid quenching, leading to unique nanostructures with enhanced properties [6]. For example, research has identified the role of laser parameters and solvents in controlling the metastable hexagonal close-packed (HCP) and face-centered cubic (FCC) nickel (Ni) nanoparticles, which exhibit enhanced electrocatalytic performance, compared to stable face-centered cubic (FCC) Ni nanoparticles, toward the hydrogen evolution reaction (HER) [6]. Furthermore, the ability to produce a wide variety of nanostructures, including nanorods, spindles, tubes, and complex shapes[7]. PLAL has been used to produce plasmonic nanoparticles, which are essential for applications in sensing and biomedicine due to their unique optical properties. Moreover, semiconductor nanoparticles synthesized by PLAL have shown significant potential for the degradation of organic pollutants, thus highlighting the environmental benefits of this technique [8].

The scalability of PLAL towards industrial applications is another critical aspect of this method. The ability to control the synthesis process (by adjusting laser parameters and the choice of liquids) opens possibilities for large-scale production of nanomaterials with tailored properties. This scalability is crucial for meeting the demands of various industries, including catalysis, energy storage, and environmental remediation [8].

The solvents influence the ablation process and the resulting nanostructures due to their different physicochemical properties, such as viscosity and polarity, and the thickness, size, and quality of the graphene sheets can be controlled by adjusting the laser settings [9].

Nanoparticles are formed in different ways at various stages of the ablation process. First, a thin layer of molten metal is formed where the laser plume meets the liquid. This layer then breaks into

large nanoparticles. At the front of the growing bubble in the liquid, small nanoparticles are quickly formed and grow. Additionally, the laser plume breaks apart into many tiny nanoparticles, which then bump into each other and merge to form even smaller nanoparticles [10].

The longer laser ablation times can create more layers of 2D materials like graphite, allowing for precise control over its structure. [11].

In a top-ablation PLAL set-up, the laser beam passes through a liquid medium before reaching the target material, resulting in refraction and self-focusing effects that necessitate precise focal length adjustments based on the liquid's refractive index[12]. This setup creates a complex interaction between the laser, liquid, and target, captured by time-resolved high-speed imaging that reveals the dynamics of bubble formation and material ejection—key phases in understanding ablation mechanisms. As the laser beam traverses the liquid, its intensity decreases due to its absorption and scattering, following the Beer-Lambert law. For absorbing materials, the optical penetration depth is inversely proportional to the absorption coefficient. Upon striking the target, the laser generates a shockwave through rapid energy deposition and material expansion, and the energy flux across this wave is critical for comprehending the mechanical effects, such as material deformation and removal, during ablation. These insights are essential for optimizing PLAL processes in material science[13].

2. Experimental Details

2.1 Synthesis of MXenes Ti_3C_2Tx

1. Preparation of Ti_3AlC_2: The process begins with Ti_3AlC_2, a layered material in the MAX phase family, consisting of alternating layers of titanium carbide and aluminum. This MAX phase precursor is typically prepared by sintering a mixture of titanium, aluminum, and carbon powders

at high temperatures, forming a stable structure in which aluminum layers are sandwiched between titanium carbide sheets.

2. Etching Process to Remove Aluminum: To produce Ti_3C_2Tx MXene, the aluminum layers in Ti_3AlC_2 need to be selectively removed. This removal is achieved by using a chemical etching process. The most common etchant is hydrofluoric acid (HF), which selectively dissolves the aluminum, leaving behind a layered structure of titanium carbide. For enhanced safety, in-situ HF generation is an alternative to using HF directly. This involves combining a fluoride salt, such as lithium fluoride (LiF), with hydrochloric acid (HCl), which reacts to produce HF in a controlled manner. This approach minimizes direct handling of HF and enables the production of MXene with a clay-like consistency, which is easier to process.

3. Following the etching process, the resulting material is thoroughly washed to remove any residual acid and reaction byproducts. This step involves multiple cycles of centrifugation with deionized water until the pH of the solution stabilizes at approximately 6.

4. Delamination**:** This step involves breaking apart the layers to achieve single-layer MXene sheets. Sonication is often applied at this stage to assist in the complete delamination, resulting in a colloidal suspension of single-layer $Ti_3C_2T_x$ flakes.

5. Drying and storing the MXene: Finally, the delaminated Ti_3C_2Tx MXene is vacuum-dried at low temperature to ensure stability and prevent oxidation. It is essential to store MXene in an inert environment to maintain its properties, such as its high conductivity, as it is prone to oxidation when exposed to air.

The synthesis of Ti_3C_2Tx MXenes begins with the preparation of the Ti_3AlC_2 MAX phase, a layered material composed of alternating titanium carbide and aluminum layers. The MAX phase

is typically produced by sintering a mixture of titanium, aluminum, and carbon powders at high temperatures. To convert Ti_3AlC_2 into $Ti_3C_2T_x$ MXene, aluminum layers are selectively removed through chemical etching, commonly using hydrofluoric acid (HF) or in situ HF generation with a fluoride salt and hydrochloric acid, which enhances safety and ease of handling.

Delamination follows, where the interlayer spacing is increased and sonication is applied to separate single-layer flakes, resulting in a colloidal suspension of $Ti_3C_2T_x$ MXene. Finally, the delaminated MXene is vacuum-dried at low temperatures to ensure stability and prevent oxidation. It is essential to store the MXene in an inert environment to maintain its high conductivity and prevent degradation due to oxidation.

This streamlined process—from etching to delamination—yields high-quality $Ti_3C_2T_x$ MXene flakes with controlled characteristics, minimal defects, and exceptional properties, making them highly effective for various technological applications, including energy storage[14,15].

2.2 Laser Ablation of Ti_3AlC_2 for MXene Synthesis

The synthesis of $Ti_3C_2T_x$ MXene nanoparticles via PLAL involves directing high-energy excimer laser pulses onto a submerged Ti_3AlC_2 MAX phase target, producing nanoparticles through rapid ablation and quenching. This process can be broken down into three main stages:

The excimer laser's high photon energy at a 193 nm UV wavelength, 5 Hz repetition rate induces intense localized heating on the submerged Ti_3AlC_2 target, vaporizing surface material to form a high-temperature plasma plume. The surrounding liquid rapidly cools the plume and facilitates the trapping of nonequilibrium, or metastable, phases. The rapid energy deposition and quenching

create a unique environment that supports the formation of phases that are typically unstable under ambient conditions.

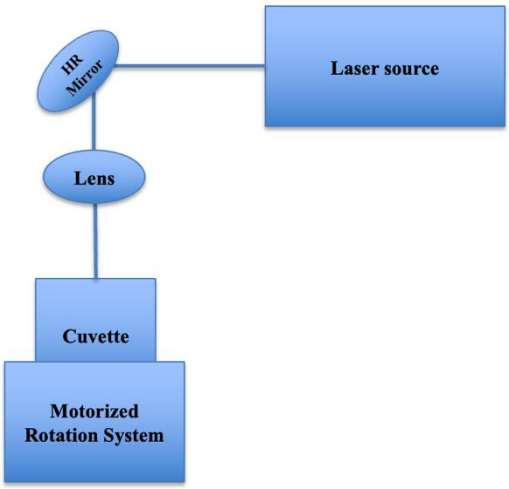

Figure 1. Schematic representation of the Pulsed Laser Ablation in Liquid (PLAL) setup used for synthesizing MXene nanostructures.

Within the plasma plume, as the material cools, nucleation begins, and primary clusters form. These clusters grow by aggregation, assisted by the cavitation bubbles generated by the laser pulse's rapid vaporization. These bubbles provide localized environments with temperatures around 1000 K and pressures up to 10^7–10^8 Pa [16], promoting unique nucleation and growth patterns. The high cooling rate afforded by the liquid quenches the hot plasma quickly and preserves metastable atomic arrangements that exhibit enhanced material properties.

The cooling and quenching within the liquid restrict atomic mobility, leading to the formation of nanostructures with high surface areas and capturing metastable phases with unique electrochemical and catalytic properties. These phases are particularly desirable for applications in energy storage as they enhance conductivity and capacitance.

For efficient energy absorption and uniform ablation, the Ti_3AlC_2 target typically measures around 1–2 mm in thickness. This ensures consistent interaction with the laser beam and minimizes heat dissipation into the bulk material.

A water depth of 10 mm above the target provides stability for cavitation bubbles and allows the laser energy to reach the target with minimal refraction. Sodium Dodecyl Sulfate (SDS), added at a concentration of 0.5 g/L, serves as a surfactant to prevent nanoparticle aggregation. SDS stabilizes freshly formed particles by imparting a negative surface charge, which repels particles from each other and reduces reaggregation, leading to more uniform nanoparticle dispersions.

Using a focal length of approximately 30 cm helps to concentrate the laser energy effectively on the target's surface, optimizing ablation while minimizing scattering losses. This control is crucial for the excimer laser's high-energy UV pulses and ensures a consistent and efficient ablation process.

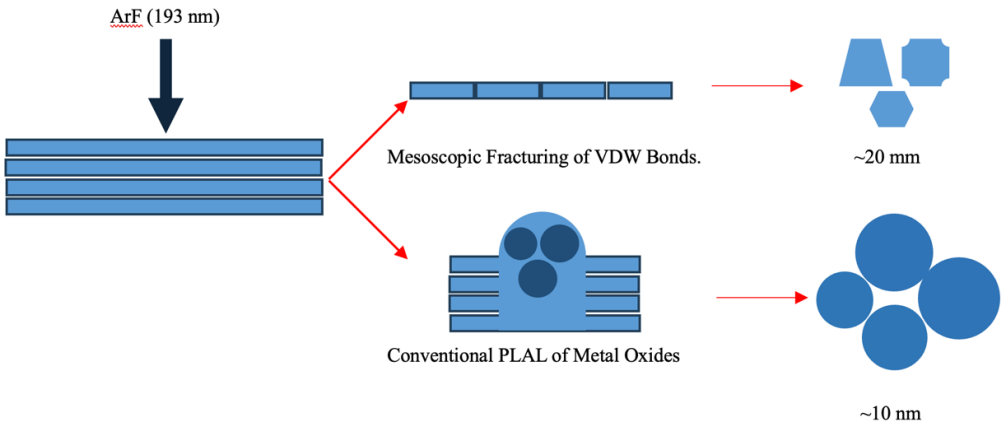

Figure 2. Illustration of the effects of an ArF excimer laser (193 nm) during Pulsed Laser Ablation in Liquid (PLAL) on layered materials: (1) Mesoscopic fracturing of Van der Waals (VDW) bonds, resulting in exfoliation into ~20 nm-sized layers, and (2) Conventional PLAL fragmentation of metal oxides, producing ~10 nm-sized nanoparticles through cavitation and plasma-induced processes.

When an excimer laser, such as an ArF laser at 193 nm with the fluence of 2-4 J/cm^2, is used for PLAL, it interacts with layered materials, leading to two primary effects as illustrated in the diagram:

1. Mesoscopic Fracturing of Van der Waals Bonds:

The high-energy laser pulse can break the weak Van der Waals (VDW) bonds between layers of the material. This results in exfoliation, where individual or few layers of the material are separated.

2. Conventional PLAL of Metal Oxides:

The laser energy not only breaks bonds but also generates cavitation bubbles and plasma, causing further fragmentation into smaller nanoparticles. These nanoparticles are typically spherical and measure around ~10 nm in size.

Impact of Anisotropic Heat Dissipation:

The layered structure leads to faster heat dissipation along the plane of the material but slower dissipation perpendicular to the layers. This anisotropy causes localized heating, making it easier to exfoliate layers without completely disrupting their structure (as seen in Figure 1). For complete nanoparticle formation, the slower heat dissipation out-of-plane contributes to the melting and rapid quenching required for creating smaller particles. The exfoliated flakes are ideal for applications requiring large surface areas, like catalysis or energy storage, while the smaller nanoparticles are better suited for applications such as drug delivery or optical devices.

1.3 Experimental Methods

The synthesis of MXenes ($Ti_3C_2T_x$) was followed by detailed characterization to confirm their structural and morphological properties. The morphology and structure of the synthesized MXenes were characterized using Scanning Electron Microscopy (SEM). This method confirmed the formation of high-purity MXene nanostructures, which are suitable for energy storage applications.

The results underscore the effectiveness of PLAL in producing nanomaterials with controlled properties, including uniformity in morphology and minimal defects. Energy Dispersive Spectroscopy (EDS), integrated with SEM, was used to validate the elemental composition, confirming the absence of significant impurities and minimal oxidation.

3. Results and Discussion

The Scanning Electron Microscopy (SEM) results for the synthesized $Ti_3C_2T_x$ MXene provide a comprehensive view of the morphology and quality of the nanostructures produced by PLAL. At various magnifications, the SEM images reveal several important characteristics of the MXene structure:

The SEM images exhibit a characteristic layered, sheet-like morphology, typical of MXenes, with clearly defined edges and minimal roughness. This layering is essential for MXenes' functional properties, as it provides high surface area and efficient ion transport pathways, crucial for energy storage applications.

In different SEM magnifications (Figure 3), the MXene flakes appear uniform in thickness and structure, suggesting that the PLAL technique effectively produces homogeneous particles. This uniformity is crucial for applications that require consistent performance, such as in batteries and supercapacitors, in which particle size and layer regularity affect conductivity and ion diffusion.

The edges of the MXene sheets are sharp and largely intact, with minimal evidence of fragmentation or damage. This observation indicates that PLAL—a rapid, high-energy process—can generate MXene sheets with preserved structural integrity. The intact edges also play a role in maintaining electrical conductivity and mechanical strength as they reduce the likelihood of defect formation that could degrade performance.

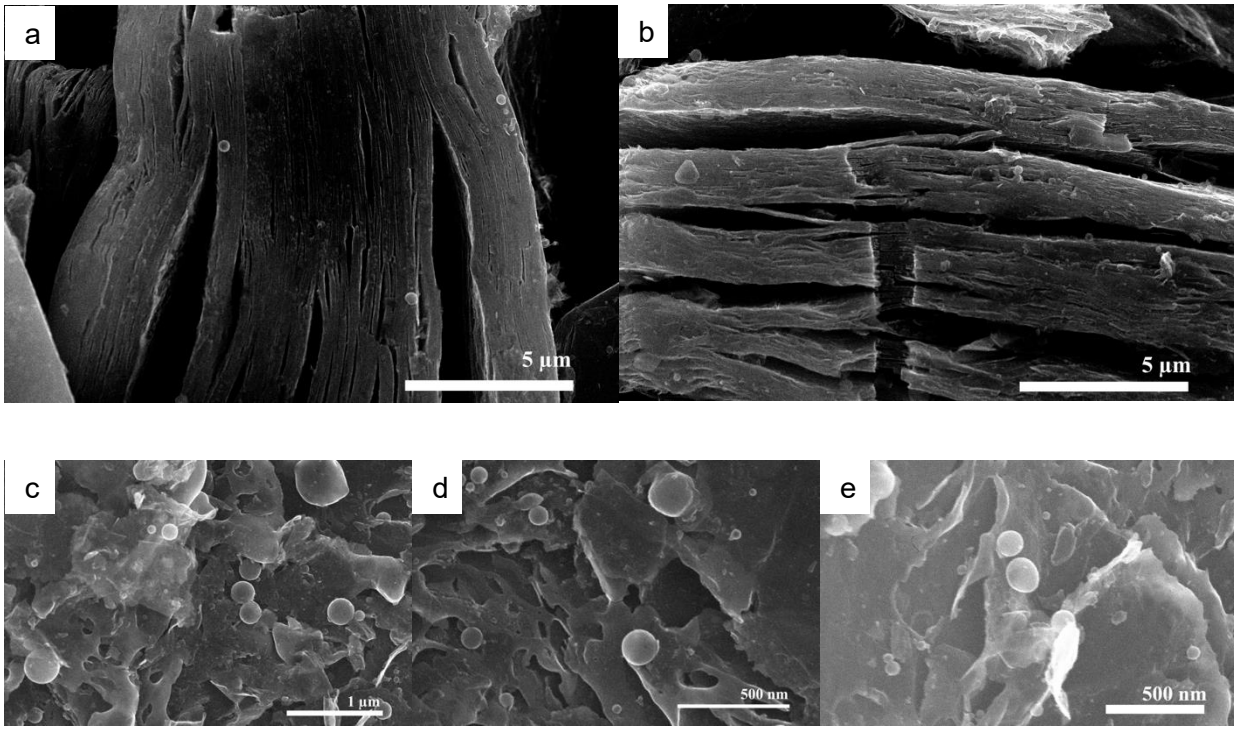

Figure 3. SEM images of Ti_3C_2 MXene nanoparticles synthesized via PLAL at different magnifications. (a) The layered structure of MXene sheets. (b) Cross-sectional SEM image displaying the stacked morphology of MXene layers. (c) Highlighting the presence of spherical nanoparticles. (d) Showing wrinkles and sheet-like structures. (e) Revealing nanoparticle distribution on the MXene sheets.

The accompanying Energy Dispersive Spectroscopy (EDS) analysis Table 1 shows a high presence of titanium (Ti) and carbon (C), the primary elements in Ti_3C_2. Only trace amounts of oxygen (O) are detected, suggesting limited oxidation during the PLAL process. This low oxygen content is advantageous, as oxidation can compromise the conductive properties of MXenes by introducing

resistive oxide layers. The minimal presence of impurities like silicon or sulfur further emphasizes the purity of the sample, highlighting PLAL's effectiveness in maintaining structural and compositional integrity.

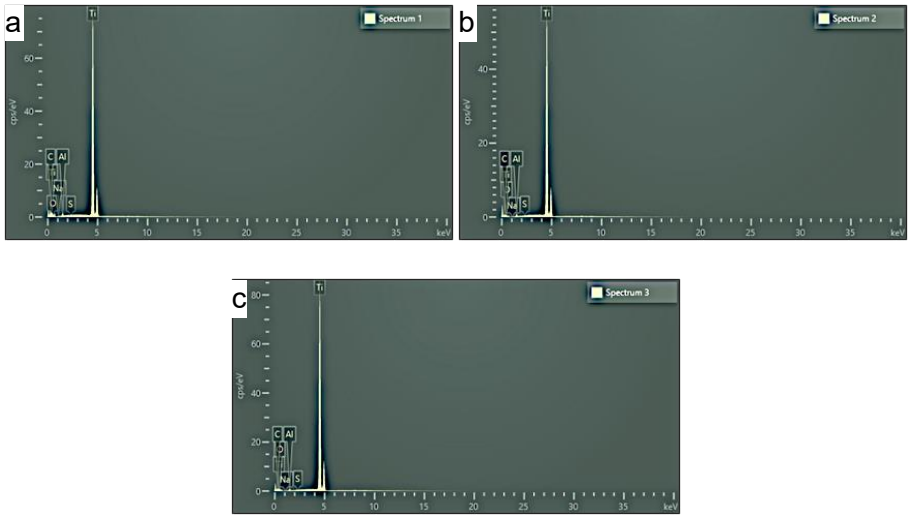

Figure 4: EDS result. (a) EDS Spectrum of Ti_3C_2 MXene Sample Showing Carbon and Titanium Peaks. (b) EDS Spectrum of Ti_3C_2 MXene Sample Indicating Minimal Oxygen Content. (c) EDS Spectrum Confirming Low Impurity Levels in the Synthesized MXene

Table 1: EDS analysis

Element	Figure 4(a)	Figure 4(b)	Figure 4(c)	Average
C	3.59	1.65	2.10	2.45
O	0.00	0.45	0.61	0.35

Na	0.01	0.00	0.01	0.01
S	0.00	0.00	0.00	0.00
Al	0.09	0.11	0.08	0.09
Ti	3.00	3.00	3.00	3.00

The SEM and EDS results collectively suggest that PLAL minimizes oxidation, likely due to the rapid cooling and quenching effects within the cavitation bubbles formed during the ablation process. This rapid cooling helps to preserve the MXene's metallic conductivity by preventing the formation of non-conductive oxide layers, critical for optimizing electrochemical performance in energy storage devices.

The uniform structure, high purity, and minimal oxidation observed in these SEM images underscore the potential of PLAL-produced MXenes for advanced energy storage applications. The layered structure enhances ion storage capacity, while the retained conductivity and minimized impurities support efficient electron transport, making these MXenes promising candidates for batteries and supercapacitors.

4. Conclusions

In conclusion, the SEM and EDS analyses together confirm that PLAL produces MXene nanostructures with excellent structural integrity, low impurity levels, and desirable morphological characteristics, reinforcing its suitability as a synthesis method for high-performance energy storage materials. The minimal oxygen content indicates limited surface oxidation, preserving the conductive properties of the material. These results highlight PLAL's potential as a scalable, contamination-free method for producing MXene-based energy storage materials with superior electrical conductivity and chemical stability. The findings demonstrate that PLAL is a reliable

and tunable synthesis approach, suitable for next-generation energy storage technologies. Future work will focus on optimizing PLAL parameters and expanding its applications across various technological fields.

Funding

Tulane University Start Up funding

Acknowledgements

We sincerely appreciate the support and contributions of Professor Naguib and his research lab for their invaluable assistance in the synthesis of MXene, which was fundamental to this project. Their resources significantly enhanced the quality of our research, and we are deeply grateful for their guidance and collaboration.

We would also like to extend our gratitude to our collaborators for their insightful discussions and constructive feedback, which have enriched this work.

References:

(1) Nyabadza, A.; Vazquez, M.; Brabazon, D. A Review of Bimetallic and Monometallic Nanoparticle Synthesis via Laser Ablation in Liquid. *Crystals* **2023**, *13* (2), 253. https://doi.org/10.3390/cryst13020253.

(2) Yogesh, G. K.; Shukla, S.; Sastikumar, D.; Koinkar, P. Progress in Pulsed Laser Ablation in Liquid (PLAL) Technique for the Synthesis of Carbon Nanomaterials: A Review. *Appl. Phys. A* **2021**, *127* (11), 810. https://doi.org/10.1007/s00339-021-04951-6.

(3) Acharyya, J. N.; Gangineni, R. B.; Rao, D. N.; Prakash, G. V. Photonic and Electronic State Interactions in BaTiO3 Based Optical Microcavity. **2021**.

(4) Yan, Z.; Chrisey, D. B. Pulsed Laser Ablation in Liquid for Micro-/Nanostructure Generation. *J. Photochem. Photobiol. C Photochem. Rev.* **2012**, *13* (3), 204–223. https://doi.org/10.1016/j.jphotochemrev.2012.04.004.
(5) Mafuné, F.; Kohno, J.; Takeda, Y.; Kondow, T. Formation of Stable Platinum Nanoparticles by Laser Ablation in Water. *J. Phys. Chem. B* **2003**, *107* (18), 4218–4223. https://doi.org/10.1021/jp021580k.
(6) Park, C. E.; Jeong, G. H.; Theerthagiri, J.; Lee, H.; Choi, M. Y. Moving beyond Ti2C3Tx MXene to Pt-Decorated TiO2@TiC Core–Shell via Pulsed Laser in Reshaping Modification for Accelerating Hydrogen Evolution Kinetics. *ACS Nano* **2023**, *17* (8), 7539–7549. https://doi.org/10.1021/acsnano.2c12638.
(7) Elafandi, S.; Ahmadi, Z.; Azam, N.; Mahjouri-Samani, M. Gas-Phase Formation of Highly Luminescent 2D GaSe Nanoparticle Ensembles in a Nonequilibrium Laser Ablation Process. *Nanomaterials* **2020**, *10* (5), 908. https://doi.org/10.3390/nano10050908.
(8) Fazio, E.; Gökce, B.; De Giacomo, A.; Meneghetti, M.; Compagnini, G.; Tommasini, M.; Waag, F.; Lucotti, A.; Zanchi, C. G.; Ossi, P. M.; Dell'Aglio, M.; D'Urso, L.; Condorelli, M.; Scardaci, V.; Biscaglia, F.; Litti, L.; Gobbo, M.; Gallo, G.; Santoro, M.; Trusso, S.; Neri, F. Nanoparticles Engineering by Pulsed Laser Ablation in Liquids: Concepts and Applications. *Nanomaterials* **2020**, *10* (11), 2317. https://doi.org/10.3390/nano10112317.
(9) Yogesh, G. K.; Shukla, S.; Sastikumar, D.; Koinkar, P. Progress in Pulsed Laser Ablation in Liquid (PLAL) Technique for the Synthesis of Carbon Nanomaterials: A Review. *Appl. Phys. A* **2021**, *127* (11), 810. https://doi.org/10.1007/s00339-021-04951-6.
(10) Shih, C.-Y.; Shugaev, M. V.; Wu, C.; Zhigilei, L. V. The Effect of Pulse Duration on Nanoparticle Generation in Pulsed Laser Ablation in Liquids: Insights from Large-Scale Atomistic Simulations. *Phys. Chem. Chem. Phys.* **2020**, *22* (13), 7077–7099. https://doi.org/10.1039/D0CP00608D.
(11) Pramanik, A.; Karmakar, S.; Kumbhakar, P.; Biswas, S.; Sarkar, R.; Kumbhakar, P. Synthesis of Bilayer Graphene Nanosheets by Pulsed Laser Ablation in Liquid and Observation of Its Tunable Nonlinearity. *Appl. Surf. Sci.* **2020**, *499*, 143902. https://doi.org/10.1016/j.apsusc.2019.143902.
(12) Subedi, R.; Guisbiers, G. Synthesis of Ultrawide Band Gap TeO_2 Nanoparticles by Pulsed Laser Ablation in Liquids: Top Ablation versus Bottom Ablation. *ACS Omega* **2024**, *9* (24), 25832–25840. https://doi.org/10.1021/acsomega.3c10497.
(13) Yan, Z.; Chrisey, D. B. Pulsed Laser Ablation in Liquid for Micro-/Nanostructure Generation. *J. Photochem. Photobiol. C Photochem. Rev.* **2012**, *13* (3), 204–223. https://doi.org/10.1016/j.jphotochemrev.2012.04.004.
(14) Naguib, M.; Barsoum, M. W.; Gogotsi, Y. Ten Years of Progress in the Synthesis and Development of MXenes. *Adv. Mater.* **2021**, *33* (39), 2103393. https://doi.org/10.1002/adma.202103393.
(15) Alhabeb, M.; Maleski, K.; Anasori, B.; Lelyukh, P.; Clark, L.; Sin, S.; Gogotsi, Y. Guidelines for Synthesis and Processing of Two-Dimensional Titanium Carbide ($Ti_3C_2T_x$ MXene). *Chem. Mater.* **2017**, *29* (18), 7633–7644. https://doi.org/10.1021/acs.chemmater.7b02847.
(16) Occhicone, A.; Sinibaldi, G.; Danz, N.; Casciola, C. M.; Michelotti, F. Cavitation Bubble Wall Pressure Measurement by an Electromagnetic Surface Wave Enhanced Pump-Probe Configuration. *Appl. Phys. Lett.* **2019**, *114* (13), 134101. https://doi.org/10.1063/1.5089206.